

APPLICATION OF LAWS' MASKS TO BONE TEXTURE ANALYSIS: AN INNOVATIVE IMAGE ANALYSIS TOOL IN OSTEOPOROSIS

M. Rachidi¹, C. Chappard¹, A. Marchadier¹, C. Gadois², E. Lespessailles¹, C.L. Benhamou¹

¹ INSERM Unit 658, Orleans Hospital, Orleans, France

² D3A[®] Medical Systems, Orleans, France

Address for correspondence: Mouna RACHIDI, INSERM Unit 658, IPROS-CHR-Orleans.

1 rue Porte Madeleine. BP 2439. 45032 Orléans. Cedex 1. France.

Tel: (+33)2.38.74.40.61, Fax: (+33)2.38.74.40.24. E-mail: mouna.rachidi@chr-orleans.fr

ABSTRACT

The objective of this study was to explore Laws' masks as a new application of texture analysis to characterise bone micro-architecture and to check its dependence from the spatial resolution. The method is based on masks that aim to filter the images. From each mask, classical statistical parameters can be calculated. Our study was performed on 114 women with osteoporotic fractures and 182 age-matched healthy post menopausal women. For all subjects radiographs were obtained of the calcaneus with a new high-resolution X-ray device. The bone mineral density measurements were assessed by DXA.

The best compromise between reproducibility and capability to discriminate between fractured cases and controls were obtained with the "standard deviation" parameter derived from the TR_{E5E5} Mask. This study showed the dependence of Laws' masks parameters on image resolution, which confirms the necessity to perform Laws' textural measurements on high-resolution images.

Thus, this method seems to be a promising routine technique for the determination of osteoporosis fracture risk from radiographs of the calcaneus independently from BMD.

KEY WORDS: Laws' masks; Trabecular bone; Texture analysis; Calcaneus radiographs; Osteoporosis

1. INTRODUCTION

Osteoporosis is a bone disorder that leads to increased fracture risk. It was defined by the World Health Organisation as a decrease of bone mass and a deterioration of bone microarchitecture [1]. In our laboratory, we have developed and validated different textural parameters to assess bone quality on calcaneus radiographs [2]: the fractal analysis [3], the degree of anisotropy [4], and co-occurrence and grey level run-length matrices [5]. Our paper presents a new method: the texture energy measurements developed by Kenneth Ivan Laws [6] are known as one of the best methods for texture analysis in image processing, and are used in various applications, including medical image analysis [7,8]. They were used to detect defects in ceramic tiles [9], for texture analysis in spatial images [10]. In medical image analysis, they were used on intravascular ultrasound and dermatological images [11], our study is the first application of these masks to trabecular bone

characterisation on high-resolution digital X-ray images of the calcaneus in vivo. The first objective of our study was to determine whether Laws' masks were relevant to describe structural variations of trabecular bone due to osteoporosis on high-resolution digital images. The second one was to examine the dependence of Laws' masks parameters on spatial resolution evaluated by voluntary degradation of the resolution.

2. MATERIALS AND METHODS

2.1 Subjects

The protocol was a uni-center case-control study of postmenopausal women recruited from the Orleans Hospital Center. It was performed on 182 healthy post menopausal women (72.5 ± 11.4 years) with no fracture and 114 age-matched women with fractures (70.3 ± 9.5 years). Bone mineral density (BMD) (g/cm^2) from the lumbar spine (LS-BMD), femoral neck (FN-BMD), and total hip (TH-BMD) were measured by dual-energy X-ray absorptiometry (Delphi, Hologic, Waltham, MA).

For all subjects the radiographs of the calcaneus were obtained with a new high-resolution X-ray device with direct digitisation (BMATM, D3A[®], Medical System, Orleans, France). The acquisitions were obtained with the following characteristics: Focal distance 1.15 m and X-ray parameters 55 kV and 20 mAs. The high-resolution digital detector integrated into this prototype had a $50 \mu\text{m}$ pixel size, providing a spatial resolution of 8 line pairs per millimetre at 10% modulation transfer function [5]. On each radiograph a similar region of interest (ROI) of 256 pixels x 256 pixels was located in an area of trabecular bone defined by two anatomical landmarks (**fig. 1**) [12]. Then, Laws' masks were used to extract texture parameters from the ROI.

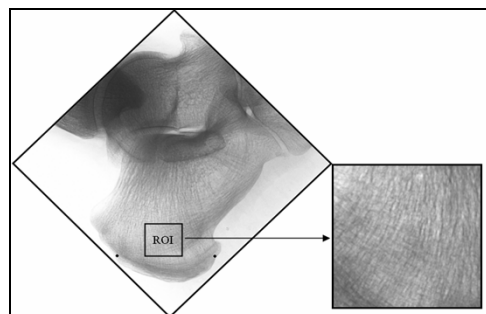


Fig.1: Region of interest for texture analysis on the calcaneus radiograph images with anatomical landmarks

To evaluate the quality of image required for the extraction of the texture features, we simulated a decrease in the resolution of the image. We changed pixel size, which corresponded to the true resolution, but nothing was modified on the measuring equipment. The simulation was computed by the averaging of 4, 16, or 64 pixels (initial pixel size=50 μ m). Thus, the image resolutions obtained were, respectively, 100, 200 and 400 μ m.

2.2 Texture features extraction by Laws' masks

The method is based on texture energy transforms applied to the image to estimate the energy within the pass region of filters [6]. All the masks were derived from one-dimensional (1-D) vectors of five pixels length: L₅, E₅, S₅, W₅, R₅, respectively, describe the following features: level, edge, spot, wave and ripple (fig.2).

E ₅ (Edge) = [-1 -2 0 2 1] → Edge detection
L ₅ (Level) = [1 4 6 4 1] → Level detection
S ₅ (Spot) = [-1 0 2 0 -1] → Spot detection
R ₅ (Ripple) = [1 -4 6 -4 1] → Ripple detection
W ₅ (Wave) = [-1 2 0 -2 -1] → Wave detection

Fig.2: Five 1-D Laws' vectors

By convoluting any vertical one-dimensional vector with a horizontal one, 25 two-dimensional filters of size 5x5 were generated (fig.3):

L ₅ L ₅	E ₅ L ₅	S ₅ L ₅	W ₅ L ₅	R ₅ L ₅	L ₅ E ₅	E ₅ E ₅
S ₅ E ₅	W ₅ E ₅	R ₅ E ₅	L ₅ S ₅	E ₅ S ₅	S ₅ S ₅	W ₅ S ₅
R ₅ S ₅	L ₅ W ₅	E ₅ W ₅	S ₅ W ₅	W ₅ W ₅	R ₅ W ₅	L ₅ R ₅
E ₅ R ₅	S ₅ R ₅	W ₅ R ₅	R ₅ R ₅			

Fig.3: Twenty five 2-D Laws' masks

To extract texture information from an image I_(i,j), the image was first convoluted with each two-dimensional mask. For example, if we used E5E5 to filter the image I_(i,j), the result was a "texture image" (TI_{E5E5}) (Eq.1):

$$TI_{E5E5} = I_{(i,j)} \times E_5 E_5 \quad (1)$$

According to Laws, all the two dimensional masks, except L₅L₅ had zero mean. Thus, texture image TI_{L5L5} was used to normalize the contrast of all other texture images TI_(i,j) (Eq.2). This step made these descriptors contrast independent.

$$Normalize(TI_{Mask}) = \frac{TI_{(i,j)Mask}}{TI_{(i,j)L5L5}} \quad (2)$$

The outputs (TI) from Laws' masks were passed to "texture energy measurements" (TEM) filters. These consisted of a moving non-linear window average of absolute values (Eq.3).

$$TEM_{(i,j)} = \sum_{u=-7}^7 \sum_{v=-7}^7 |TI_{(i+u,j+v)}| \quad (3)$$

By combining the twenty five TEM descriptors, we obtained fourteen rotationally invariant texture energy measurements (noted TR). For example TR_{E5L5} was obtained as follows:

$$TR_{E5L5} = \frac{TEM_{E5L5} + TEM_{L5E5}}{2}$$

TR _{E5E5}	TR _{E5L5}	TR _{E5R5}	TR _{E5S5}	TR _{E5W5}
TR _{L5R5}	TR _{L5S5}	TR _{L5W5}	TR _{R5S5}	TR _{R5W5}
TR _{R5W5}	TR _{R5R5}	TR _{S5S5}	TR _{W5W5}	

Fig.4: Fourteen Rotationally Invariant texture energy measurements

Finally, from each TR we computed five statistical parameters: "mean", "standard deviation", "entropy", "skewness" and "kurtosis".

2.3 Statistical analysis

All statistical tests were performed with the statistical analysis software NCSS (2004). Student's t-test was employed to compare mean values between cases and control groups. The significance level was chosen at p ≤ 0.05. Correlation analysis between texture parameters versus age and BMD were performed using Pearson or Spearman coefficients according to samples distribution. An ANCOVA analysis was used to take into account the possible effect of covariant factors, such as age and TH-BMD.

2.4 Precision assessment

Reproducibility calculations were expressed as the root mean square average coefficient of variation (RMSCV %) [13]. To calculate the in vitro reproducibility, thirty-three images were obtained on phantom of calcaneus without repositioning. To determine in vivo short-term precision error the heel of thirty healthy women (58.2 ± 6.8 years) was imaged twice with repositioning. For the in vivo mid-term precision error, fourteen subjects (44.2 ± 14.4 years) underwent three measurements at 1-week intervals [5].

3. RESULTS

In terms of reproducibility, the best results were obtained with TR_{E5E5} and TR_{E5L5} masks, especially for three parameters: "mean", "standard deviation" and "entropy" with, respectively, in vitro RMSCV% = 1.01 [95% CI, 0.65-1.77], 1.50 [95% CI, 0.97-2.63] and 1.15 [95% CI, 0.74-2.01] for TR_{E5E5}, and 1.16 [95% CI, 0.76-2.04], 1.32 [95% CI, 0.86-2.32] and 1.31 [95% CI, 0.85-2.29] for TR_{E5L5}. The lowest values were obtained for the TR_{E5S5} mask. The highest values were obtained for TR_{E5R5} and TR_{E5W5} masks. As showed in table 1 the most interesting parameter was "standard deviation" derived from the TR_{E5E5} mask, which separated controls from fractures cases.

	p-value	
	TR _{E5E5}	TR _{E5L5}
"mean"	NS	NS
"standard deviation"	4x10 ⁻⁴	2.6x10 ⁻³
"entropy"	NS	NS

Table 1: Statistical Comparisons of parameters derived from TR_{E5E5}, TR_{E5L5} masks between controls and fractures cases (α = 0.05) (NS not significant)

Moreover, controls and groups with fractures were largely discriminated after adjustment for age and TH-BMD individually and adjusted for both ($p=5 \times 10^{-5}$). There were no significant correlation between texture parameter “standard deviation” and age, body mass index (*BMI*) or BMD measurements.

In addition, we studied relationship between the “standard deviation” parameter for the TR_{E5E5} mask at $50\mu\text{m}$ and at several resolutions (100, 200 and $400\mu\text{m}$) between controls and fractures cases. **Table 2** expresses the results of this correlation test and the calculation of the standard error of the estimate (*SEE*).

Resolution	Equation	R ²	SEE
100 μm	2.17X - 0.04	0.80	0.06
200 μm	2.53X - 0.04	0.47	0.35
400 μm	1.71X - 0.03	0.38	1.27

Table 2: Results of correlation test and the standard error of the estimate (*SEE*) between “standard deviation” parameter (TR_{E5E5} mask) at $50\mu\text{m}$ and at several pixel size

Table 3 represents the in vitro RMSCV% of the same parameter “SD”, and a statistical comparison between groups as a function of image resolutions. These data showed a statistically significant difference between groups at 50 and $100\mu\text{m}$ of resolution, but at 200 and $400\mu\text{m}$ the statistical difference was lost.

	50 μm	100 μm	200 μm	400 μm
RMSCV%	1.50	3.76	3.43	9.26
95% CI	0.97 –	2.43 –	2.22 –	5.99 -
p	2.63×10^{-2}	6.58×10^{-2}	NS	NS

Table 3: In vitro RMSCV% and statistical comparison of “standard deviation” parameter (TR_{E5E5} mask) between controls and fractures cases according to image resolution

4. DISCUSSION

This method has shown its ability to discriminate fracture women from controls, independently from BMD measurements with reasonable reproducibility. The best parameter was “Standard Deviation” obtained from TR_{E5E5} mask. It was the first time that Laws’ masks had been used in trabecular bone characterisation on bone images.

In vivo, few imaging techniques are available to assess bone microarchitecture such as peripheral quantitative computed tomography (*pQCT*) [14], magnetic resonance imaging (*MRI*) [15]. These techniques are not widely available and have little potential to be used on large populations. Radiographic assessment is well suited to assess trabecular bone microarchitecture on two dimensional projection images because of its ease of use and availability. The technique of radiographs has the advantage of being able to be used on large populations. For the current study, we used high-resolution radiographs in vivo directly digitised on C-MOS detector [5]. The direct digitisation process has the advantage of reducing the number of steps leading to the final result, and, consequently, of reducing the variations linked to these different steps, so the reproducibility can be improved [5].

Different types of trabecular bone texture analysis have been assessed. Fractal analysis provides a reflection of the image roughness and characterises the self-similarity of the texture grey-level variations over different scales [3,16]. Statistical texture analysis based on co-occurrence and grey level run-length matrices, describe the inter-relationships of the grey levels of neighbour pixels [5].

In several applications, Laws’ method is considered to be of interest for extracting texture characteristics of the images. In endovascular ultrasound imaging of the carotids, the “energy” and “entropy” parameters have been recognised to differentiate atheromatous plates on TR_{E5L5} , TR_{L5S5} and TR_{E5S5} masks [17]. In a similar study, the “mean”, “variance” and “range of values” on the TR_{E5L5} mask were found to be pertinent to recognise calcified, fibrous and necrotic core plates [7]. The different image properties underlined by different masks depend on the type of images. In comparison with high-resolution bone X-rays images, ultrasound images have a low resolution, with speckle noise and non-uniform luminance and contrast [7]. In bone tissue characterisation, Smyth et al. [18] used Laws’ method to analyse the texture of the proximal femur on radiographs with the aim of ranking them in comparison with the Singh grading system used by radiologists. They concluded that Laws’ features provided a better classification than did an untrained observer.

Laws’ masks were used for global texture extraction, aiming to describe general texture properties from each image [19]. Starting from the fourteen masks used, we have chosen five of them: TR_{E5E5} , TR_{E5L5} , TR_{E5S5} , TR_{E5R5} and TR_{E5W5} , which have a normal distribution of data. Secondly, we retained the “standard deviation” “mean” and “entropy” parameters on the TR_{E5E5} and TR_{E5L5} masks which produced the best reproducibility measurements. Finally, “standard deviation” on the TR_{E5E5} is probably the best parameter to separate women with fractures from control cases. These results are in agreement with those described by Laws who determined that “variance” and “standard deviation” were the best parameters to extract texture information from images [20]. The Laws’ masks seem able to detect subtle variations between textured images. The visual pattern of trabecular bone images either from osteoporosis cases or from control cases is quite similar (fig.4), while the convolution by the TR_{E5E5} Laws’ mask reveals obvious differences in the image. These differences reflect probably trabecular microarchitecture variations, concerning trabecular thickness, spacing, number, and connectivity.

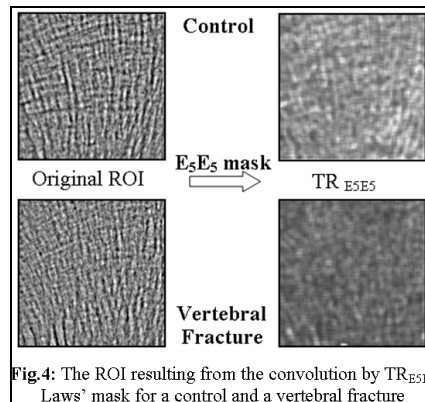


Fig.4: The ROI resulting from the convolution by TR_{E5E5} Laws’ mask for a control and a vertebral fracture

Our results showed the dependence of Laws' masks texture parameters on image resolution. With a pixel size twice that of the initial image (initial pixel size=50 μ m), we obtained quite reasonable results in terms of reproducibility and ability to separate fracture cases from controls. When the pixel size was increased over 200 μ m, the information contained in the images was lost. These results demonstrate the necessity to perform Laws' masks textural measurements on high-resolution images.

Most of the texture analyses require a filtering process to limit the influence of low-frequency variation due to soft tissue [4,5]. Generally, it is preferable to limit as far as possible the pre-treatment process, direct analysis offers the advantage of retaining the maximum information present in the images [2]. The application of the Laws' masks requires no image pre-processing. This point constitutes one of the advantages of this technique.

5. CONCLUSION

This study showed the ability of Laws' masks to reveal pertinent information concerning trabecular bone texture on high-resolution images, and confirmed the independence and complementary of these textural parameters to bone mineral density. Thus, Laws' masks may constitute one of the best methods for bone texture analysis.

REFERENCES

[1] NIH Consensus Development Panel on Osteoporosis Prevention, Diagnosis, and Therapy, *Osteoporosis Prevention, Diagnosis, and Therapy*, JAMA. 285 (2001) 785-795.

[2] C.L. Benhamou, Texture analysis on bone radiographs, *Bone Quality Seminars, Osteoporosis Int.*, vol. 18, pp. 864-867, 2007.

[3] C.L. Benhamou, S. Poupon, E. Lespessailles, et al. Fractal analysis of radiographic trabecular bone texture and bone mineral density: two complementary parameters related to osteoporotic fractures. *JBMR*, vol.16, pp. 697-704, 2001.

[4] C. Chappard, B.B. Imbault, G. Lemineur, et al. Anisotropy changes in post-menopausal osteoporosis: characterization by a new index applied to trabecular bone radiographic images. *Osteoporosis Int.* vol. 16, pp. 1193-1202, 2005.

[5] E. Lespessailles, C. Gadois, G. Lemineur, et al, Bone Texture Analysis on Direct Digital Radiographic Images: Precision Study and Relationship with Bone Mineral Density at the Os Calcis, *Calcif Tissue Int.*, vol. 80, pp. 97-102, 2007.

[6] K.I. Laws, Textured image segmentation, PhD Dissertation, University of Southern California. Los angles, California 1980.

[7] D.G. Vince, K.J. Dixon, R.M. Cothren, and J.F. Cornhill, Comparison of texture analysis methods for the characterization of coronary plaques in intravascular ultrasound images, *Computerized Medical Imaging and Graphics*, vol. 24, pp. 221-229, 2000.

[8] C.I. Christodoulou, C.S. Pittichis, M. Pantziaris, and A. Nicolaides, Texture based classification of atherosclerotic carotid plaques, *IEEE Trans Med. Imaging*, vol. 22, pp. 902-912, 2003.

[9] H.A. Habib, M.H. Yousaf, and M. Mohibullah, Modified Laws Energy descriptor for inspection of ceramic tiles, National conference on Emerging Technologies, 2004.

[10] M. Singh and S. Singh, Spatial texture analysis: a comparative study, *Pattern Recognition, Proceedings, 16th International Conference*, vol. 1, pp. 676 – 679, 2002.

[11] M. Ananthaa, R.H. Mossb, and W.V. Stoecker, Detection of pigment network in dermatoscopy images using texture analysis, *Computerized Medical Imaging and Graphics*, vol. 28, pp. 225-234, 2004.

[12] C.L. Benhamou, E. Lespessailles, G. Jacquet, et al, Fractal organisation of trabecular bone images on calcaneus radiographs, *JBMR*, vol. 9, pp. 1909-1918, 1994.

[13] C.C. Gluer, and G. Blake, Accurate assessment of precision errors: How to measure the reproductibility of bone densitometry techniques, *Osteoporosis Int.*, vol. 5, pp. 262-270, 1995.

[14] V. Bousson, QCT, Pqct, microCT, and bone architecture, *Bone Quality Seminars, Osteoporosis Int.*, vol. 18, pp. 867-871, 2007.

[15] F.W. Wehrli, Characterization of bone microarchitecture by MRI in vitro an in vivo, *Bone Quality Seminars, Osteoporosis Int.*, vol. 18, pp. 850-859, 2007.

[16] T.J Vokes, M.L. Giger, M.R. Chinander, et al, Radiographic texture analysis of densitometer-generated calcaneus images differentiates postmenopausal women with and without fractures, *Osteoporosis Int.*, vol. 17, pp. 1472–1482, 2006.

[17] S.Gr. Mougiakakou, S. Golimati, I. Gousias, A.N. Nicolaides, and K.S. Nikita, Computer-aided diagnosis of carotid atherosclerosis based on ultrasound image statistics, Laws' texture and neural networks, *Ultrasound in Med. & Biol.*, vol. 33, pp. 26–36, 2007.

[18] P.P. Smyth, J.E. Adams, R.W. Whitehouse, and C.J. Taylor, Application of computer texture analysis to the Singh index, *The British Journal of Radiology*, vol. 70, pp. 242-247, 1997.

[19] M. Rachidi, A. Marchadier, C. Gadois, et al, Laws' Masks descriptors applied to Bone Texture Analysis: an Innovative and Discriminant Tool in Osteoporosis, Accepted at *Skeletal Radiology*.

[20] D.E. Haris, Texture analysis of skin cancer images, Doctorate in Electrical Engineering Dissertation, University of Missouri-Rolla, 1994.